Sigma J Eng Nat Sci, Vol. 43, No. 2, pp. 441−451, April, 2025

Sigma Journal of Engineering and Natural Sciences
Web page info: https://sigma.yildiz.edu.tr
DOI: 10.14744/sigma.2025.00000

Research Article

Automatic identification of brittle, elongated and equiaxed ductile fracture modes in weld joints through machine learning

K. GAJALAKSHMI[1], S. SARAVANAN[2,*]

[1]*Independent Researcher*
[2]*Department of Mechanical Engineering, Annamalai University, Tamilnadu, 608002, India*

ARTICLE INFO

Article history
Received: 09 February 2024
Revised: 20 March 2024
Accepted: 26 April 2024

Keywords:
Confusion Matrix; GLCM; LBP; SVM; Wavelet Transform; Weld Fracture

ABSTRACT

Identification of the fracture mechanism in weld joints is essential for ensuring weld quality, reduce weld defects, along with enhancing the welding process. Therefore, an attempt is made to use image processing techniques such as wavelet transformation, Gray-Level Co-occurrence Matrix (GLCM), and Local Binary Pattern (LBP) to develop an automatic identification system for brittle, elongated, and equiaxed ductile fracture modes in weld joints. The GLCM technique employ Haralick functions, while the LBP and wavelet transform techniques use histograms and Gabor filters, respectively for extracting features in the fracture images. Classification based on textural features (granular or fiberous) was performed using support vector machine. LBP achieved superior accuracy of 96%, followed by GLCM. Further research could explore real-time implementation and expand the dataset to enhance the system's robustness and applicability.

Cite this article as: Gajalakshmi K, Saravanan S. Automatic identification of brittle, elongated and equiaxed ductile fracture modes in weld joints through machine learning. Sigma J Eng Nat Sci 2025;43(2):441−451.

INTRODUCTION

Welding, an indispensable process in industries, encompass a wide array of processes tailored to suit specific applications viz., automotive, aerospace, construction, and manufacturing. The welding methodologies such as arc welding, gas welding, resistance welding, or laser welding, is chosen based on material, design, and environmental conditions [1]. The efficient welding operation hinge upon the meticulous optimization of parameters to attain enhanced weld quality, weld strength, and structural integrity thereby defects and production costs are reduced [2]. The intricate relationship between welding parameters and weld strength is dictated by the nature of failure. The failure mechanisms, failure modes, and the impact of welding parameters are determined by analyzing the fracture images [3].

In this consequence, automatic categorization of the fracture mode is significant, and is characterized by the nature of texture formed on the surface. The most prevalent fracture modes in the weld joints subjected to monotonic loading are brittle (B), elongated ductile (El) and equiaxed (EQ) ductile [3]. The brittle fracture displays a smooth and flat texture that appears to be glossy or shiny. Meanwhile,

***Corresponding author.**
*E-mail address: ssvcdm@gmail.com

This paper was recommended for publication in revised form by Editor-in-Chief Ahmet Selim Dalkilic

Published by Yıldız Technical University Press, İstanbul, Turkey

the ductile fracture exhibits a rough fibrous texture and a stable propagation of grains. The fiberous grains with spherical or cuboidal shapes without any discernible elongation along any axis are equiaxed ductiles, whereas the grains that are elongated along any axis are termed as elongated ductile. However, categorization of fracture modes in scanning electron microscope (SEM) images is tedious, as they are uneven, and contain variable illumination levels across the image [4]. Traditionally, visual inspection which is simple and quick is employed to classify the fracture modes. However, it is prone to bias and hence unsuited for quantitative analysis. In this context, the use of image processing techniques is an effective approach to automatically detect and classify the fracture modes [5].

The integration of neural network based artificial intelligence (AI) techniques revolutionized welding by enabling predictive modeling, process control, and defect detection with higher accuracy [6]. Neural network based techniques aids in analyzing datasets comprising welding parameters, material properties, and defect characteristics and facilitates real time decision making and adaptive control. Recently, researchers adopted convolutional neural networks (CNNs) and other deep learning architectures, capable of identifying and classifying defects such as porosity, cracks, and weld discontinuities in real time [7]. The relevant research pertaining to the application of image processing on fracture analysis is summarized in the next section.

Related Work

In an earlier study, Weng attempted to mathematically define fractures by edge detection [8]. In this context, Souza et al. introduced the machine learning algorithm (GLCM) to identify the ferritic steel morphologies in the low carbon steel weld fusion zone [9]. Meanwhile, Dutta et al. successfully extended the GLCM technique to identify fracture modes in austenitic stainless steel based on texture variation [10]. In another study, Naik and Kiran employed the LBP technique to develop a mechanism for automatic identification of fracture surfaces [4]. Lu et al. recently compared experimental and analytical fracture classification methods in metals and found that the analytical method (Ridgelet-Kernel Principal Component Analysis) extracts non-linear data more effectively [11]. In a different attempt of classifying three cast iron (malleable, white, and ductile) grades using GLCM and LBP techniques, Gajalakshmi et al. advocated the LBP method for superior classification [12].

To successfully detect friction stir welding defects such as voids, cracks, grooves, flash, and keyholes, Ranjan et al. utilized the image pyramid and image reconstruction techniques [13]. They deployed support vector machines, neural networks and k-NN in weld radiography images. Likewise, Moreno et al. used the random forest method to successfully classify porosity in aluminum metallographic images [14]. The salient research contributions in weld defects using image processing techniques are summarized in Table 1.

Although image processing was applied in the past to identify defects and classify fractures in metals, studies on the detection and classification of fractures in weld joints are scarce. Hence, weld fracture images of similar and dissimilar alloys are classified using machine learning techniques

Table 1. Methodologies and research gaps in weld defect analysis

Authors	Methods	Approaches	Difficulties
Valentin et al. [15]	GLCM and LBP in weld defect detection	Identified weld defects with 95% accuracy. GLCM provided better discrimination of defect textures.	Limited focus on analyzing the effect of various wavelet functions on noise reduction
Bastidas-Rodriguez et al. [16]	Fracture analysis of metal structures Using GLCM and wavelet transform	Wavelet transform enhanced the ability to detect micro-cracks	Limited analysis
Jayasudha and Lalithakumari [17]	Weld defect detection using GLCM and Wavelet Transform	Successfully detected weld defects with 93% accuracy. Wavelet captured subtle variations in texture.	Role of LBP in feature extraction is not explored
Patil and Thote [18]	Analysis of microstructure defects in welds using GLCM and wavelet transform	Identified microstructural defects in welds with 92% accuracy.	Limited investigation into the effect of varying GLCM parameters on feature extraction
Prasad et al. [19]	Weld defect detection using GLCM and LBP features enhanced by wavelet transform	Detected weld defects with 94% accuracy. Combined GLCM and LBP features provided better discrimination of defect patterns. Wavelet transform improved image clarity.	Lack of investigation into the effect of different wavelet thresholding techniques on noise reduction
Karthikeyan et al. [20]	Texture Analysis of Weld Fractures using GLCM, LBP, and Wavelet Transform	Integrated GLCM, Combined use of GLCM, LBP, and Wavelet transform provided superior texture characterization.	Limited exploration of the computational efficiency of the combined feature extraction methods

such as Wavelet transform, GLCM, and LBP, and the results are presented.

Wavelet transformation captures both global and local texture features effectively making it suitable for identifying subtle defects such as cracks, pores, and weld bead irregularities. Moreover, wavelet-based features are robust to noise and illumination variations, ensuring reliable defect detection in challenging environments. Likewise, GLCM is a texture analysis method that characterizes the spatial relationships of pixel intensities in an image. By quantifying the occurrence of pairs of pixel intensity values at specified spatial offsets, GLCM generates a comprehensive set of statistical features that encapsulate textural properties such as contrast, homogeneity, and entropy. These features are particularly valuable for discriminating between different materials and surface textures, making GLCM well-suited for defect detection in welding images. By encoding the local texture variations into binary patterns, LBP facilitates the extraction of discriminative texture features robust to changes in illumination and noise. In the context of defect detection in welding images, LBP offers several advantages, including computational efficiency, simplicity of implementation, and insensitivity to image transformations [12].

MATERIALS AND METHODS

- Two hundred images of each fracture mode are collected from Annamalai University, India to create a dataset.
- In addition, the fracture images of tensile (ASTM E-8), and ram tensile (MIL-J-24445A standard) and the shear (ASTM B 898 standard), and Charpy impact (ASTM E23-16b standard) obtained from our previous explosive cladding [21-23] and laser butt welding [24, 25] are added to the dataset.
- The sample fracture images comprising brittle, elongated, and equiaxed ductile are depicted in Fig.1 (a-i). In weld joints, brittle fractures have a distinct shiny, flat surface that often demonstrates distinct signs of crack propagation. The stretched appearance of elongated ductile fractures in the direction of applied force indicates plastic deformation before collapse. The shape of an equiaxed ductile fracture is more uniform and rounded, indicating that deformation occurred uniformly in all directions [26-28].
- Machine learning techniques which involve three steps viz., fracture image collection, feature extraction, and classification, are implemented on the acquired fracture images [29].
- Subsequently, the fracture images are converted into a gray scale images to increase the contrast, during the preliminary pre-processing stage.
- In addition, random variations in pixel values in the image are removed and resized to 240 X 240 pixels.
- Finally, feature extraction using the wavelet transform, GLCM, and LBP techniques is implemented by a Matlab 2020b code performed in a Intel Core-i5 personal computer.
- The fractures in the weld fractograph images are characterized by the prevalence of different textures viz. progressive or radial or river-like ones.
- Subsequently, a Support Vector Machine (SVM) is employed to categorize the extracted features and the classification performance is measured using a confusion matrix and F-score.
- The methodology adopted in the present study is schematically shown in Fig.2 and the description of the attempted feature extraction algorithms is given below.

Wavelet Transform

A sinusoidal signal with a specific frequency and orientation modulated by a Gaussian wave is the basis of a 2D Gabor filter. A bank of Gabor filters with various orientations is used to analyze the texture or to extract features from an image. Real and imaginary sections of the filter are used to represent orthogonal directions. The two sections may be combined into a complex number or utilized separately [30].

Gray Level Co-Occurrence Matrix

The Grey Level Co-occurrence Matrix (GLCM) executes an operation following the second-order statistics in the images, to identify the textural relationship between a pair of pixels. GLCM analyzes different combinations of pixels and establishes the frequency of the pixel pairs based on brightness [15-19]. Based on the gray value of the image, the GLCM characteristics are displayed as a matrix having a similar number of rows and columns. The components of the matrix depend on the frequency of the two specific pixels and pixel pairs differ with respect to their neighborhood. Depending on the gray value of the rows and columns, the values of the matrix hold the second-order statistical probability values. The transient matrix is quite large if the intensity values are larger [20]. GLCM features such as autocorrelation, contrast, correlation, cluster prominence, cluster shade, dissimilarity, energy, entropy, homogeneity, maximum probability, sum of squares, sum average, sum variance, sum entropy, difference variance, difference entropy, information measure of correlation, inverse difference normalized, and inverse difference moment normalized are used in this study. These features are used to construct a GLCM feature matrix that can successfully represent an image with fewer parameters.

Rotation Invariant and Histogram Fourier LBP

LBP describes the texture of an image based on the sign variations between neighboring and center pixels. A binary code is generated for each pixel in the image by thresholding its neighbor with the central pixel value, termed binary patterns. The neighboring pixel becomes "1" if its value is greater than or equal to the threshold value and "0" if its value is lower. Subsequently, the frequency values of binary patterns are calculated using the histogram. Each pattern indicates a potential binary pattern detected in the image. The number of pixels utilized in the LBP computation determines the number of histograms [19].

SVM for Classification

Support vector machine (SVM), a supervised machine learning algorithm, classifies the image by training and testing of data, and plays a vital role in image classification. A classification task involves training and testing of data that contain some data instances. Each instance in the training set contains one target value and several features. The objective of SVM is to produce a model that predicts the target value of data instances in the testing set, with features alone as input [31]. Target values or known labels indicate whether the system is performing satisfactorily or not, which points to a desired response, validating the accuracy of the system, or be used to help the system to learn and perform in a desired way.

Performance Measurement

The correlation between the predicted and the actual image that occurs is reported as either positive (P) or negative (N). The three weld fracture modes viz., brittle, elongated ductile, and equiaxed ductile are distinguished by labels G1, G2, and G3 respectively. In addition to the above two classifications, a true positive (TP) is counted if the model predicts the positive, a false negative (FN) is an outcome where the model predicts the negative correctly. A true negative (TN) is counted if the occurrence is negative and is designated as such; a false positive (FP) is counted if the model incorrectly predicts the positive class. The measurement parameters such as precision (closeness of two or more measurements to each other), accuracy (closeness of the measured value with the true value), recall (marginal mean consistency error), specificity (probability of a negative result, conditioned on the individual truly being negative.) and F-score (a measure of a model's accuracy on a dataset) are calculated by [12].

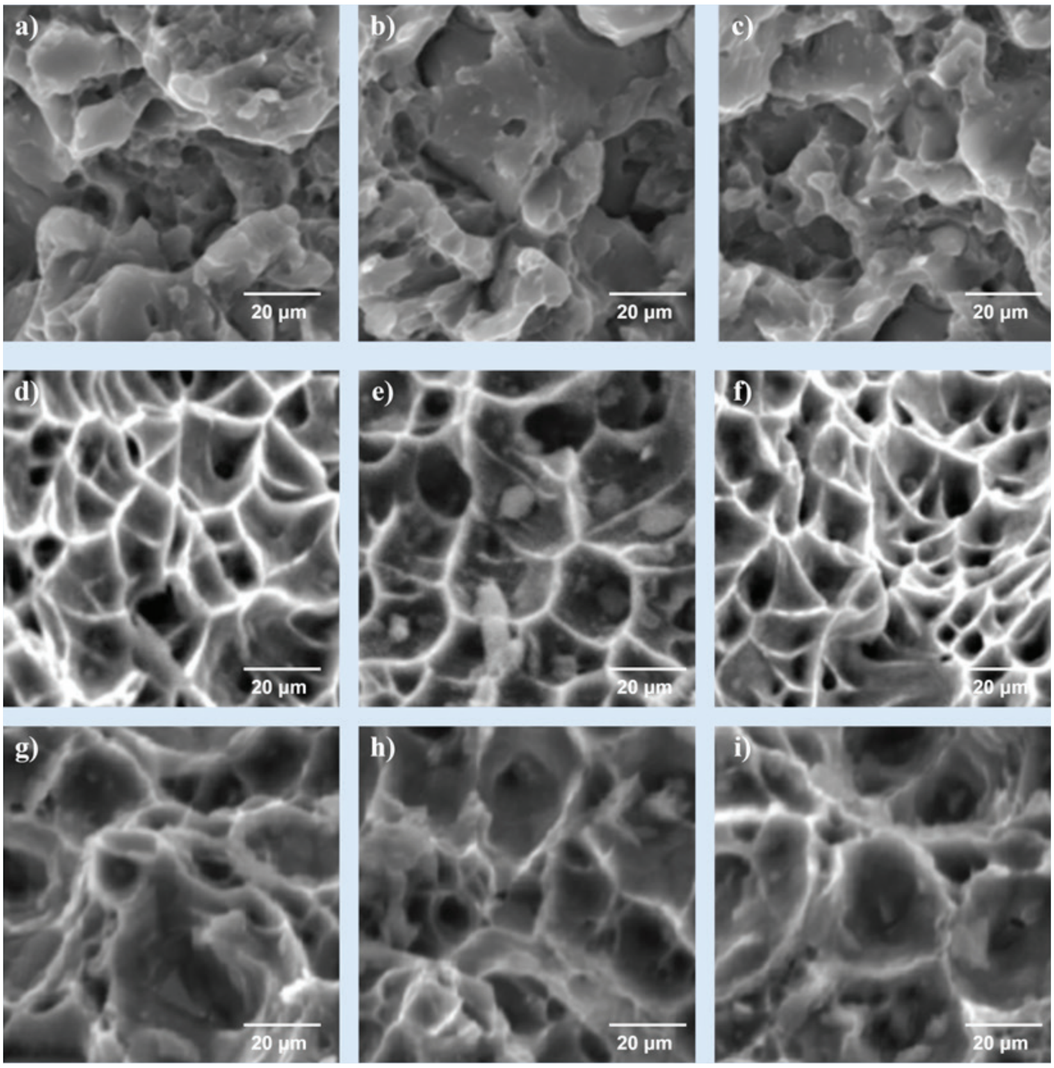

Figure 1. Weld fracture images (a) Brittle (b) Equiaxed ductile and (c) Elongated ductile.

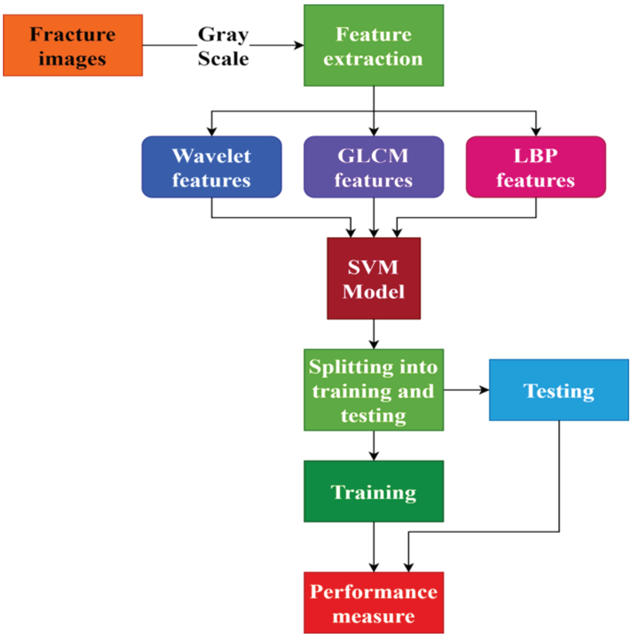

Figure 2. Methodology.

$$Precision = \frac{TP}{(TP+FP)} \qquad (1)$$

$$Recall = \frac{TP}{(TP+FN)} \qquad (2)$$

$$Accuracy = \frac{TP+TN}{P+N} \qquad (3)$$

$$Specificity = \frac{TN}{(TN+FP)} \qquad (4)$$

$$F-Score = \frac{2}{(1/(precision+1/recall))} \qquad (5)$$

RESULTS AND DISCUSSION

Feature Extraction by Wavelet Transform

The feature identifies textures in an image based on the prevailing overall or average spatial relationship among the pair of pixels in the gray tones at a certain distance and angle [32]. By requantizing the original image into a gray image, a feature with 32 levels is created. Identical to the original images, wavelet transform creates pixels with a coefficient of 240x240. The coefficients in the matrix determine the continuity of pixels at angles 0, 45, 90, and 135 degrees. The feature extraction in wavelet transform is implemented by determining the difference of mean value in each row of the image. If the difference in mean value is less than 5, continuity prevails and hence is marked as "1". If the mean value is greater than 5, it is set to zero, indicating the absence of continuity. The features extracted by wavelet transform in brittle, equiaxed ductile and elongated ductile weld fracture are shown on the left side of the fracture images in Figs.3-5.

Wavelet Transform captures the continuity of pixels and highlights the variations prevailing in the mean values of the gray image and also analyzes the coefficients at different angles (Brittle fracture: 1818028, 3453311, 4512326, 3930515, 2188499, 188028, 3453311, 452326, 3930515). This method is capable of distinguishing brittle, equiaxed ductile, and elongated ductile fractures, providing valuable information about fracture morphology based on microstructural features.

Feature Extraction by GLCM

In GLCM, the pre-processed gray image is segmented by edge detection and thresholding. Subsequently, boundaries are thinned and the GLCM values are calculated at four different angles (00, 450, 900 and 1350) by the gray co-matrix function, which represents the horizontal intimacy between pixels. The four key Haralick [33] features viz., energy, entropy, correlation, and contrast, displayed on the 3 x 3 sample matrix [21:25 1:5] extracted from each image are shown on the sides of the microstructure in

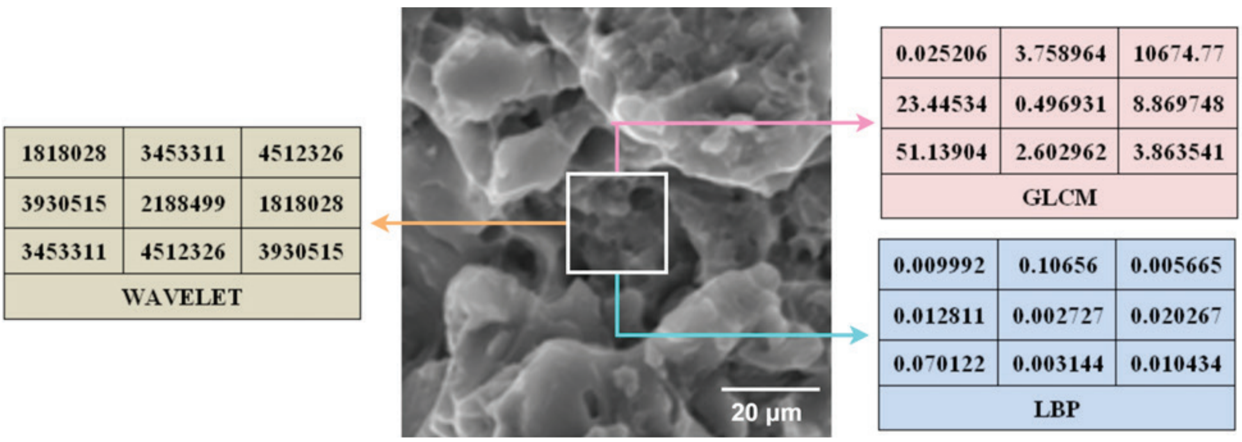

Figure 3. Features extracted from a brittle weld fracture image.

Figs.3-5 (Elongated ductile: 0.025206, 3.758964, 10674.77, 23.44534,.496931, 8.869748, 51.1394, 2.602962, 3.863541). The variation in correlation, energy, entropy, and dissimilarity features exhibit slight variations across the three weld fracture modes. Hence, the additional thirteen Haralick features such as normalization energy, sum of variance, information measure of correlation, sum variance, sum average, different variance, inverse different moment, and difference entropy attributes are calculated to characterize the image textures and to prepare a feature set of the weld fracture modes. A deeper analysis of texture variations across different fracture modes is rendered possible by additional computation of Haralick features, which increases the discriminative ability of GLCM.

Feature Extraction by LBP

In LBP, a circle is placed on the input gray image and the values of the center pixel are compared with the surrounding eight pixels prevailing at an equal angle of 45 degrees (left-top, left-middle, left-bottom, right-top, etc.). If the value of the neighboring pixel is larger or equal to the central pixel, "1" is marked, otherwise, "0." Thereby, eight decimal values are obtained from each circle of an input image, yielding 238 X 238 values. The binary code obtained is considered as the binary pattern. After obtaining the binary values, the generated circle is moved from one region to another with the aid of the bit shift function. The mean value of the binary code obtained in the whole image (Equiaxed dimple: 0.09286, 0.002242, 0.044742, 0.002149, 0.069487, 0.064296, 0.003799, 0.009393, 0.001123) is shown on the right side of the fractographs (Figs.3-5). If there are no more than two 0-1 or 1-0 transitions, LBP is referred to as uniform. Uniform patterns are more stable and less susceptible to noise, hence yielding credible estimates from small numbers of samples [34]. Ojala et al. [35] categorized texture based on the neighboring eight and sixteen pixels, observed 90% and 70% uniform patterns, respectively. However, the pixels having more than two transitions (non-uniform patterns) and groups are not considered in this study.

After obtaining values from the whole image, a histogram is computed based on the values obtained on the whole image. The histogram highlights the frequency of binary patterns in the chosen image. To increase the extraction

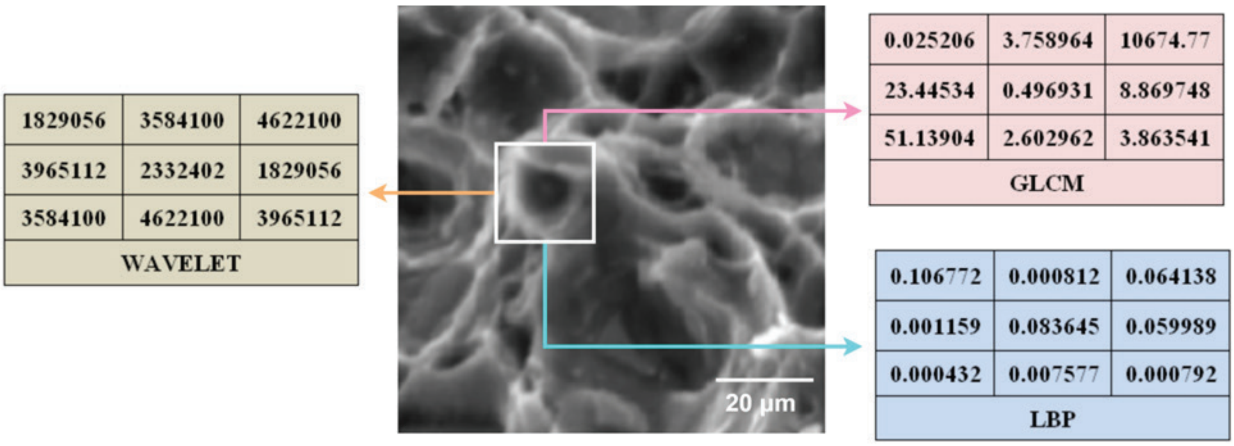

Figure 4. Features extracted from an elongated ductile weld fracture image.

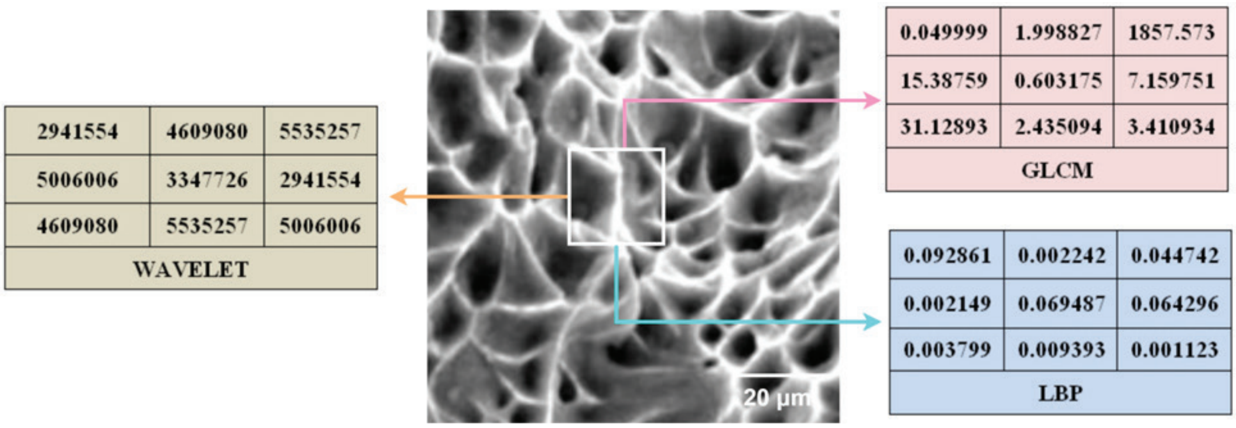

Figure 5. Features extracted from equiaxed ductile weld fracture image.

speed and performance and to reduce the dimensionality consistent patterns are used to describe textures.

After execution, the original weld fracture image is rotated by 90o, and the same steps are repeated to acquire an additional 59 uniform pattern image features. The Fast Fourier Transform (FFT) determines the 38 most significant features, after removing repetitive and insignificant characteristics that describe the image texture. The integration of FFT further enhances the feature extraction by identifying the most significant patterns in the fracture image [36]. By focusing on repetitive and high-impact characteristics, FFT streamlines the feature vector and reduces dimensionality, facilitating more efficient classification of weld fracture modes. This highlights the importance of feature selection in optimizing the performance of support vector machines (SVM).

Training and Evaluation

The weld fractures are represented as Grade 1 for brittle (weld fracture without appreciable prior plastic deformation), Grade 2 for elongated ductile (formation and collection of microvoids along the granular boundary of the alloy), Grade 3 for equiaxed ductile (spherical depressions that coalesce normal to the loading axis). The SVM classifier is trained via the features obtained from the wavelet, GLCM, and LBP techniques utilizing the SVMTorch tool employing the leave-one-out (LOO) algorithm in the K-fold strategy. As suggested by Di Martino and Sessa [37], three alternative combinations of training and testing were performed using threefold methods. Eighty percent of the 600 images in the database are utilized for training, while the remaining 20% are used for testing. After training and testing, the effectiveness of the model is assessed by evaluating its accuracy.

The confusion matrix, which requires two dimensions, was employed for determining the values of FP, TP, TN, and FN. The first dimension is the actual grade determined by human experts (as established by manual inspection), and the other is the outcome of the prediction. A test set of features that were left out of the training set is used to assess the classifier's performance. So, the classifier runs five times using the K-fold approach, taking 120 images from the database each time. The overall accuracy of the model is determined as the average of the cross-validations. The confusion matrix (Table 2) illustrates the classification effectiveness of the developed approach concerning each weld fracture mode.

The ability to identify weld fracture modes plays a vital role in ensuring structural reliability and safety of the weld joints.The proposed feature extraction methods provide new insights into the different weld fracture images and has its own merits and demerits. The optimal feature extraction method is chosen based on its classification accuracy. However, other criteria such as ease of use, interpret the results, efficiency, and processing times have to be considered as well.

The wavelet transform predicts 75, 74 and 76 percent of the 600 images classified into the three weld fracture modes (Table 3: G1, G2, and G3). Due to skewed image representation and inadequate feature extraction to detect microscopic changes, brittle fracture is erroneously identified as ductile fracture. The inability of the model to capture the subtle differences between elongated and an equiaxed ductile fracture is the reason for the misclassification of elongated ductile images as equiaxed ductile fractures. In the wavelet transform, about 25% of the images were incorrectly categorized. The lower performance of wavelet transform is due to the slower shift sensitivity, poor directionality and lack of phase information. Meng et al [38] while performing image reconstruction observed similar results. The classification performance of the GLCM and LBP techniques, however, is higher than 90%. The F-score of the GLCM technique is 97, 94 and 94 percent in the detection and classification of three weld fracture modes, respectively. With respect to the GLCM's prediction performance, roughly 3% of brittle weld fractures are incorrectly identified as equiaxed ductiles or elongated ductile weld fracture modes, whereas 6% of equiaxed ductiles are incorrectly identified as brittle weld fractures or elongated ductile weld fracture modes. Moreover, LBP's classification performance (Table 3) is more accurate because it yields 97, 95, and 97 percent accurate predictions, due to its robustness to gray scale changes.

Table 2. Performance of weld fracture mode classification

Feature technique	Prediction/Actual	B	El	EQ
Wavelet	**B (G1)**	170	20	10
	El (G2)	15	165	20
	EQ(G3)	15	15	170
GLCM	**B (G1)**	190	5	5
	El (G2)	7	187	6
	EQ(G3)	3	8	189
LBP	**B (G1)**	194	3	2
	El (G2)	6	190	5
	EQ(G3)	0	7	193

Table 3. Performance metrics

Feature technique	Grade	Precision	Recall	Specificity	F-score
Wavelet	**B (G1)**	73	73	74	75
	El (G2)	76	76	75	74
	EQ(G3)	78	78	78	76
GLCM	**B (G1)**	97	98	98	97
	El (G2)	93	94	97	94
	EQ(G3)	94	95	98	94
LBP	**B (G1)**	99	99	98	97
	El (G2)	94	94	97	95
	EQ(G3)	95	95	96	97

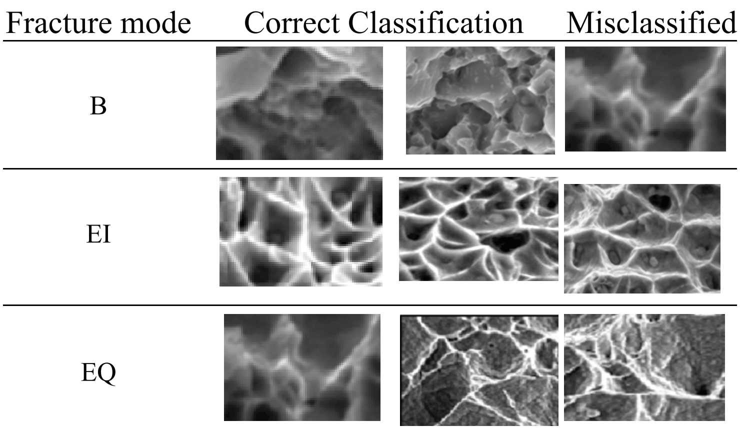

Figure 6. Classified and misclassified fracture images.

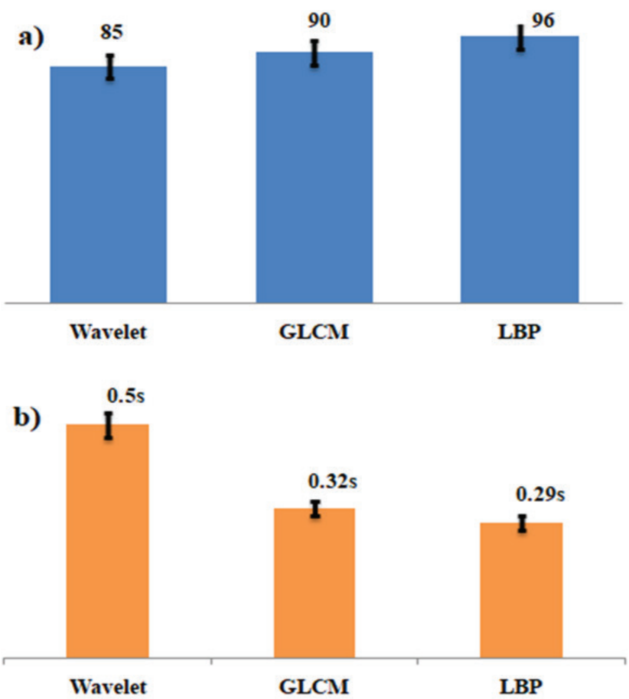

Figure 7. (a) Accuracy and (b) computational time of proposed techniques.

The higher accuracy of LBP is consistent with the studies of Garg and Dhiman [39]. The misclassification reduces to 3% and 5% respectively as the prediction of the brittle and elongated ductile is more accurate (97.0%). LBP captures texture variations at a finer scale, particularly in regions with complex microstructures. The emphasis on uniform patterns improves the robustness of texture analysis, making LBP a valuable tool for detecting subtle changes in weld fracture textures. The sample of accurate classification and misclassification, performed by the human expert, in each fracture mode is presented in Fig. 6.

After the confusion matrix, the classification performance is measured by parameters such as accuracy, F-score, precision, recall, and specificity [40]. The performance of weld fracture mode classification using wavelet, GLCM, and LBP are displayed in Table 2 and Table 3. The accuracy of classification by wavelet, GLCM and LBP are 85%, 90%, and 96% respectively (Fig.7a). In addition, the processing time of wavelet, GLCM, and LBP are (<0.5 s), as shown in Fig.7b. The closer predictions make the machine learning models to be used during weld joints fracture mode classification. By leveraging the complimentary abilities of GLCM, LBP, and wavelet transform, researchers can create robust models in the near future. These developments will eventually increase safety and dependability in engineering systems by having a substantial impact on quality control, defect identification, and failure analysis in welding applications.

CONCLUSION

Three distinct kinds of fracture modes in weld joints are classified using machine learning techniques: Wavelet, GLCM, and LBP. GLCM and LBP techniques determine the weld fracture mode in a weld joint with an efficiency of 90% and 95% respectively. Of the two techniques, LBP is superior owing to its ability to capture fine texture variations in complex microstructures. The F-score of wavelet transform ranges between 74 and 76, the same for the GLCM and LBP techniques are higher than 90, indicating their effectiveness. The computational time for LBP is much less and holds the potential for automating the process.

The future scope can be expanded by considering potential avenues for developing methods for real-time implementation of the classification algorithm and allowing for automated detection and classification of weld fracture modes during welding process. Create frameworks to integrate algorithm into the workflow processes. Collaborate with industry to validate the performance of the classification algorithm in real-world scenarios.

NOMENCLATURE

B	Brittle
EI	elongated ductile
EQ	equiaxed ductile
FN	False Negative
FP	False Positive
G1	brittle
G2	elongated ductile
G3	equiaxed ductile
GLCM	Grey Level Co-occurrence Matrix
NN	k-Nearest Neighbor
LBP	Local Binary Pattern
LOO	Leave-One-Out
N	Negative
P	Positive
SDSS	Super Duplex Stainless Steel
SEM	Scanning Electron Microscope
SVM	Support Vector Machine
TN	True Negative

AUTHORSHIP CONTRIBUTIONS

Authors equally contributed to this work.

DATA AVAILABILITY STATEMENT

The authors confirm that the data that supports the findings of this study are available within the article. raw data that support the finding of this study are available from the corresponding author, upon reasonable request.

CONFLICT OF INTEREST

The author declared no potential conflicts of interest with respect to the research, authorship, and/or publication of this article.

ETHICS

There are no ethical issues with the publication of this manuscript.

REFERENCES

[1] Padala VRR, Rao KVS. Investigation on effect of TIG welding parameters on dissimilar weld joints of AISI 304 and AISI 310 steels using response surface method. Sigma J Eng Nat Sci 2021;39:80–96.

[2] Khaliq UA, Muhamad MR, Yusof F, Ibrahim S, Isa MSM, Chen Z, Çam G. A review on friction stir butt welding of aluminum with magnesium: a new insight on joining mechanisms by interfacial enhancement. J Mater Res Technol 2023;27:4595–4624. [CrossRef]

[3] Moore PL, Booth G. The welding engineer's guide to fracture and fatigue. Amsterdam: Elsevier; 2014.

[4] Naik DL, Kiran R. Identification and characterization of fracture in metals using machine learning-based texture recognition algorithms. Eng Fract Mech 2019;219:106618. [CrossRef]

[5] Munawar HS, Hammad AW, Haddad A, Soares CAP, Waller ST. Image-based crack detection methods: a review. Infrastructures 2021;6:115. [CrossRef]

[6] Tsuzuki R. Development of automation and artificial intelligence technology for welding and inspection process in aircraft industry. Weld World 2022;66:105–116. [CrossRef]

[7] Valizadeh M, Wolff SJ. Convolutional neural network applications in additive manufacturing: a review. Adv Ind Manuf Eng 2022;4:100072. [CrossRef]

[8] Weng GR. Image processing and classification of metal fracture surface. Proc Int Conf Wavelet Anal Pattern Recognit 2008;163–167. [CrossRef]

[9] Souza AC, Silva GC, Caldeira L, de Almeida Nogueira FM, Junior MLL, de Aguiar EP. An enhanced method for the identification of ferritic morphologies in welded fusion zones based on gray-level co-occurrence matrix: a computational intelligence approach. Proc Inst Mech Eng Part C J Mech Eng Sci 2021;235:1228–1240. [CrossRef]

[10] Dutta S, Das A, Barat K, Roy H. Automatic characterization of fracture surfaces of AISI 304LN stainless steel using image texture analysis. Meas 2012;45:1140–1150. [CrossRef]

[11] Lu Y, Wang L, Pan D, Chen X. Summary of metal fracture image recognition method. J Phys Conf Ser 2021;1982:012070. [CrossRef]

[12] Gajalakshmi K, Palanivel S, Nalini NJ, Saravanan S. Automatic classification of cast iron grades using support vector machine. Optik 2018;157:724–732. [CrossRef]
[13] Ranjan R, Khan AR, Parikh C, Jain R, Mahto RP, Pal S, Pal SK, Chakravarty D. Classification and identification of surface defects in friction stir welding: an image processing approach. J Manuf Process 2016;22:237–253. [CrossRef]
[14] García-Moreno AI, Alvarado-Orozco JM, Ibarra-Medina J, Martínez-Franco E. Image-based porosity classification in Al-alloys by laser metal deposition using random forests. Int J Adv Manuf Technol 2020;110:2827–2845. [CrossRef]
[15] Valentin P, Kounalakis T, Nalpantidis L. Weld classification using gray level co-occurrence matrix and local binary patterns. Proc IEEE Int Conf Imaging Syst Tech 2018;1–6. [CrossRef]
[16] Bastidas-Rodriguez MX, Prieto-Ortiz FA, Espejo E. Fractographic classification in metallic materials by using computer vision. Eng Fail Anal 2016;59:237–252. [CrossRef]
[17] Jayasudha JC, Lalithakumari S. Weld defect segmentation and feature extraction from the acquired phased array scan images. Multimed Tools Appl 2022;81:31061–31074. [CrossRef]
[18] Patil RV, Thote AM. Smart techniques of microscopic image analysis and real-time temperature dispersal measurement for quality weld joints. In: Soft Computing in Materials Development and its Sustainability in the Manufacturing Sector. CRC Press; 2022. p. 49–72. [CrossRef]
[19] Prasad G, Gaddale VS, Kamath RC, Shekaranaik VJ, Pai SP. A study of dimensionality reduction in GLCM feature-based classification of machined surface images. Arab J Sci Eng 2024;49:1531–1553. [CrossRef]
[20] Karthikeyan S, Pravin MC, Sathyabama B, Mareeswari M. DWT-based LCP features for the classification of steel surface defects in SEM images with KNN classifier. Aust J Basic Appl Sci 2016;10:13–19.
[21] Robin LG, Raghukandan K, Saravanan S. Process parameter optimization to achieve higher impact strength in SS316 wire-mesh and SiCp reinforced aluminum composite laminates produced by explosive cladding. Met Mater Int 2021;27:3493–3507. [CrossRef]
[22] Kumar P, Ghosh SK, Saravanan S, Barma JD. Experimental and simulation studies on explosive welding of AZ31B-Al 5052 alloys. Int J Adv Manuf Technol 2023;127:2387–2399. [CrossRef]
[23] Saravanan S, Gajalakshmi K. Soft computing approaches for comparative prediction of ram tensile and shear strength in aluminum-stainless steel explosive cladding. Arch Civ Mech Eng 2022;22:42. [CrossRef]
[24] Sivagurumanikandan N, Saravanan S, Sivakumar G, Raghukandan K. Process window for Nd:YAG laser welding of super duplex stainless steel. J Russ Laser Res 2018;39:575–584. [CrossRef]
[25] Kumar GS, Raghukandan K, Saravanan S, Sivagurumanikandan N. Optimization of parameters to attain higher tensile strength in pulsed Nd:YAG laser welded Hastelloy C-276-Monel 400 sheets. Infrared Phys Technol 2019;100:1–10. [CrossRef]
[26] Bolat Ç, Akgün İC, Gökşenli A. Effect of aging heat treatment on compressive characteristics of bimodal aluminum syntactic foams produced by cold chamber die casting. Int J Metalcast 2022;16:646–662. [CrossRef]
[27] Orbulov IN, Ginsztler J. Compressive characteristics of metal matrix syntactic foams. Compos Part A Appl Sci Manuf 2012;43:553–561. [CrossRef]
[28] Bolat Ç, Akgün İC, Gökşenli A. Effects of particle size, bimodality and heat treatment on mechanical properties of pumice reinforced aluminum syntactic foams produced by cold chamber die casting. China Foundry 2021;18:529–540. [CrossRef]
[29] Bansal M, Kumar M, Sachdeva M, Mittal A. Transfer learning for image classification using VGG19: Caltech-101 image dataset. J Ambient Intell Hum Comput 2023;14:3609–3620. [CrossRef]
[30] Patil RV, Thote AM. Smart techniques of microscopic image analysis and real-time temperature dispersal measurement for quality weld joints. In: Soft Computing in Materials Development and its Sustainability in the Manufacturing Sector. CRC Press; 2022. p. 49–72. [CrossRef]
[31] Wang P, Fan E, Wang P. Comparative analysis of image classification algorithms based on traditional machine learning and deep learning. Pattern Recognit Lett 2021;141:61–67. [CrossRef]
[32] Zhou YH. Wavelet numerical method and its applications in nonlinear problems. Berlin, Germany: Springer; 2021. [CrossRef]
[33] Haralick RM, Shanmugam K, Dinstein IH. Textural features for image classification. IEEE Trans Syst Man Cybern 1973;SMC-3:610–621. [CrossRef]
[34] Aouat S, Ait-hammi I, Hamouchene I. A new approach for texture segmentation based on the gray level co-occurrence matrix. Multimed Tools Appl 2021;80:24027–24052. [CrossRef]
[35] Ojala T, Pietikäinen M, Mäenpää T. Multiresolution gray-scale and rotation invariant texture classification with local binary patterns. IEEE Trans Pattern Anal Mach Intell 2002;24:971–987. [CrossRef]
[36] Lee WK, Ratnam MM, Ahmad ZA. Detection of fracture in ceramic cutting tools from workpiece profile signature using image processing and fast Fourier transform. Precis Eng 2016;44:131–142. [CrossRef]

[37] Di Martino F, Sessa S. A classification algorithm based on multi-dimensional fuzzy transforms. J Ambient Intell Hum Comput 2022;13:2873–2885. [CrossRef]

[38] Meng X, Sun F, Zhang L, Fang C, Wang X. Visual three-dimensional reconstruction based on spatio-temporal analysis method. Electronics 2023;12:53. [CrossRef]

[39] Garg M, Dhiman G. A novel content-based image retrieval approach for classification using GLCM features and texture fused LBP variants. Neural Comput Appl 2021;33:1311–1328. [CrossRef]

[40] Farsi M. Application of ensemble RNN deep neural network to the fall detection through IoT environment. Alex Eng J 2021;60:199–211. [CrossRef]